The Mechanism of Oxidation-Induced Low-Density Lipoprotein Aggregation: An Analogy to Colloidal Aggregation and Beyond?

Shaohua Xu* and Binhua Lin†
*Department of Medicine and †James Frank Institute, The University of Chicago, Chicago, Illinois 60637 USA

ABSTRACT Atherosclerosis is a disease initiated by lipoprotein aggregation and deposition in artery walls. In this study, the de novo low-density lipoprotein aggregation process was examined. Nine major intermediates were identified in two stages of the aggregation process. In the aggregation stage, low-density lipoprotein molecules aggregate and form nucleation units. The nucleation units chain together and form linear aggregates. The linear aggregates branch and interact with one another, forming fractals. In the fusion stage, spatially adjacent nucleation units in the fractal fuse into curved membrane surfaces, which, in turn, fuse into multilamellar or unilamellar vesicles. Alternatively, some adjacent nucleation units in the fractals assemble in a straight line and form rods. Subsequently, the rods flatten out into rough and then into smooth ribbons. Occasionally, tubular membrane vesicles are formed from the fractals. The aggregation stage seems to be analogous to colloidal aggregation and amyloid fiber formation. The fusion stage seems to be characteristic of the lipid-rich lipoproteins and is beyond colloidal aggregation and amyloid fiber formation.

INTRODUCTION

Aggregation and deposition of biomolecules are believed to be the underlying cause of many human diseases, including atherosclerosis, amyloidosis, and stones in the gallbladder and kidney (Kumar et al., 1997). Atherosclerotic plaque formation in human arterial intima is believed to be initiated by the extracellular aggregation and deposition of lipoproteins trapped in the subendothelial matrix because of a leakage of the artery (Getz, 1990; Guyton and Gotto, 1992; Hoff et al., 1992; Navab et al., 1996). Structures resembling lipoprotein aggregates have been identified in human arterial intima (Guyton and Klemp, 1989; Tirziu et al., 1995), isolated from aortas with minimal intimal thickening, and have been found to contain monomeric and aggregated lipoproteins, lipid droplets, and unilamellar and multilamellar vesicles (Tertov et al., 1992; Chao et al., 1990). The lipid droplets have diameters that range from 30 to 350 nm.

Conditions that induce the lipoproteins, especially low-density lipoprotein (LDL), to aggregate in vitro have been studied extensively. These cover a broad range and can be classified into three categories, namely: chemical reagents (Cu^{2+}, H_2O_2, superoxide, nitric oxide, Ca^{2+}, and acidic pH) (Navab et al., 1996; Hoff et al., 1992; Berliner and Heinecke, 1996; Rice-Evans and Bruckdorfer, 1992; Witztum and Steinberg, 1991), biochemical reagents (lipoxygenase, myeloperoxidase, phospholipase A_2 and C, sphingomyelinase, ceramide, proteoglycans, and heparin-gelatin-fibronectin) (Xu and Tablas, 1991; Chao et al., 1992; Maor and Aviram, 1999; Hakala et al., 1999; Marathe et al., 1999; Belkner et al., 1993; Camejo, 1982), and mechanical processing (vortexing) (Khoo et al., 1990).

We focused our study on how oxidants induce LDL to aggregate. Oxidative stress is believed to be one of the major factors contributing to the formation of atherosclerotic plaques. LDL has an average molecular weight of 2.5 million and consists of a central core of approximately 1600 molecules of cholesterol ester and 170 molecules of triglycerides (Berliner and Heinecke, 1996). The core is surrounded by a monolayer of ~700 molecules of phospholipids and 600 molecules of free cholesterol, integrated into which there is an amphipathic polypeptide, apoB-100. The total number of fatty acids in an LDL particle is ~3000, and ~50% of them are polyunsaturated fatty acids (PUFAs). A range of reactive oxygen species is generated under physiologic and pathophysiologic conditions (Navab et al., 1996; Rice-Evans and Bruckdorfer, 1992). When released into plasma, these oxidants can react with lipoprotein molecules.

Elucidation of the lipoprotein aggregation mechanism requires knowledge of the structure of the intermediates formed during the aggregation process. Until now, studies of lipoprotein aggregation have relied heavily on transmission electron microscopy (TEM). TEM imaging of lipoprotein aggregates, either formed in vitro or isolated from the atherosclerotic plaque, revealed structural features such as round lipid droplets and unilamellar and multilamellar vesicles (Tirziu et al., 1995; Guyton and Klemp, 1989; Tertov et al., 1992; Chao et al., 1990). However, the de novo process of lipoprotein aggregation has not been elucidated. It is unclear whether other aggregation intermediates are generated in the process, but are not detected by electron microscopy (EM), and how these lipid droplets and vesicles are formed from monomeric lipoproteins.

Digital video microscopy (DVM) has several distinct advantages for the study of lipoprotein aggregation: (1) the aggregation reaction can be monitored continuously in buffer solution; (2) the specimen does not need to be ad-

Received for publication 27 October 2000 and in final form 21 June 2001.
Address reprint requests to Shaohua Xu, PhD, The University of Chicago, Department of Medicine, MC6080, 5841 S. Maryland Avenue, Chicago, IL 60637. Tel.: 773-702-1086; Fax: 773-702-8875; E-mail: shxu@medicine.bsd.uchicago.edu.
© 2001 by the Biophysical Society
0006-3495/01/10/2403/11 $2.00

sorbed, dried, or stained, as is required by other imaging methods; and (3) the movement of individual colloidal particles, and their interaction and aggregation, can be traced (Crocker and Grier, 1996). DVM has a resolution of 80–200 nm for moving particles. TEM has a resolution of subnanometer.

In this report, we present intermediates of LDL aggregation identified by TEM and DVM. More importantly, we found how membrane vesicles are formed from the aggregates. We elucidated whether a similar pathway underlies the pro-aggregation role of these seemingly unrelated perturbations. We compared lipoprotein aggregation with amyloid fiber formation (Xu et al., 2001) and with what is known about colloidal aggregation.

MATERIALS AND METHODS

Specimen preparation

LDL (d 1.019–1.063) was purified by preparative ultracentrifugation from human plasma according to a method described by Schumaker and Puppione (1986). LDL (0.2 mg/ml in 10 mM sodium phosphate, 150 mM NaCl, 3 mM NaN_3, pH 7.2) was mixed gently with H_2O_2 (0.3% or 88 mM) in an Eppendorf tube and was used for DVM or EM specimen preparation immediately or at a desired time point. One could use a lesser amount of H_2O_2, e.g., 8 mM, but the reaction would take 3 to 5 weeks to complete. In vivo, lipoprotein aggregates and atherosclerotic plaques are generated over years or decades. Thus, it is impractical to use oxidants at physiologic concentrations (<1 mM H_2O_2) and thus observe an oxidation reaction over such a long period. For most of the DVM experiments that require continuous observation of the aggregation process, the specimen was transferred to the DVM chamber immediately after LDL was mixed with H_2O_2. LDL incubation with Ca^{2+}, H^+, or Cu^{2+} was prepared in the same way as with H_2O_2.

DVM experiments

DVM can resolve motionless particles as small as 200 nm and moving particles as small as 60 nm (Crocker and Grier, 1996). The resolution improves if the particles are fluorescent, and lipoproteins have endogenous fluorescence (Koller, 1986). The sample sealed under glass coverslips was mounted onto a coverslip holder. Two drops of mineral oil were spread on top of the coverslip. The sample was then placed on the specimen stage under an Olympus BH2 optical microscope with an oil immersion objective (100X, N.A. = 1.40). A laser beam was used for positioning the sample sealed under the coverslip and was turned off once the microscope was focused on the sample. The specimen stage was then moved manually in the *x*- and *y*-directions until an area of interest appeared on the TV monitor. The analog video signal taken by a charge-coupled device video camera (Hitachi, Tokyo, Japan) mounted on the microscope was then recorded with a videocassette recorder (GVR-S950, Sanyo Corp., Tokyo, Japan). The real-time movies were digitized through the real-time frame grabber at a rate of 30 frames per second, transferred, and digitized with a real-time frame grabber (LG-3) installed in a Macintosh computer (Apple, Cupertino, CA). The image processing routine, implemented with the interactive data language (IDL) programming language, was developed by Crocker and Grier (1996). Unless specified, data were usually taken in a window of observation of $54 \times 40\ \mu m^2$. The observation depth was always 0.5 μm for all images.

Specimens (60 μl with or without H_2O_2) were placed in the center of microscope coverslips. A line of epoxy (ultraviolet [UV] epoxy, Norland Productions, Inc., Barrington, NJ) was placed around each sample. A thin glass coverslip was placed on top of the specimen and the epoxy glue just before exposure of the coverslips to UV light to cure the glue. The specimen was protected from UV light by a piece of aluminum foil placed on top of the upper coverslip just above the sample. A chamber 2–3 cm long, 1–1.5 cm wide, and 100–200 μm deep was formed between the glass coverslips and the solidified epoxy glue. The specimen was then sealed in the glass chamber. The oxidation and the aggregation of lipoproteins took place in the chamber. At each time point, the specimens were examined with DVM continuously for a period of 30 min. Unless specified, the specimens were analyzed between 3 and 5 p.m. every day for a consecutive 6-day period.

TEM

The TEM images were obtained with a CM120 transmission electron microscope (Phillips, Eindhoven, The Netherlands) with an LaB6 filament, a 50-μm objective aperture, and a 200-μm condenser aperture. The specimens were imaged with a low-dose electron beam generated at 120 kV at a magnification of 20,000 to 45,000. Images were recorded on Kodak SO163 film (Eastman Kodak, Rochester, NY).

Specimens (3 μl) of LDL oxidized with H_2O_2 were spread on glow-discharged 400-mesh carbon-coated copper grids (Pella Corp., Pella, IA). After 3 min of incubation allowing adsorption of the protein, the grid was rinsed with five drops of phosphate buffer for removal of unbound proteins. Five drops of staining solution (1% uranyl acetate) were applied to the grid. Excess stain was removed instantly by a gentle touch of a Kimwipe (Roswell, GA) tissue to the grid, and the grid was air-dried for 5 min before being imaged with TEM.

Terminology

Proteins are colloids. Aggregation of proteins is thus a colloidal aggregation process. The following terminology in colloidal chemistry is used in this paper. Colloid, derived from the word for glue in Greek, is used to describe those large and slow-moving particles that are suspended in a medium of a different phase, for example, clouds, smog, ink, and milk. Biomacromolecules all fall into the category of solid colloidal suspensions in an aqueous medium. The nucleation units are the basic units for aggregation. They are solid spheres made of spherical aggregation of individual protein molecules. Continuous aggregation of the nucleation units leads to the formation of curved linear aggregates and fractals. Curved linear aggregation is used to describe the one-dimensional (1-D) aggregation of nucleation units. Fractals are aggregates of nucleation units with structural features that cannot be defined mathematically with unitary dimensions, but with fractions of dimensions. Fractals can have amorphous structural features, such as snowflakes.

RESULTS

We followed the structures of various intermediates, their chronologic appearance, and their continuous change during LDL aggregation. Several chemical reagents are used to induce LDL aggregation, including oxidants, acidic pH, and dications. LDL was incubated with these chemical reagents at room temperature between two sealed glass coverslips. The specimen was then examined with DVM at a desired time point. Representative images were captured and analyzed.

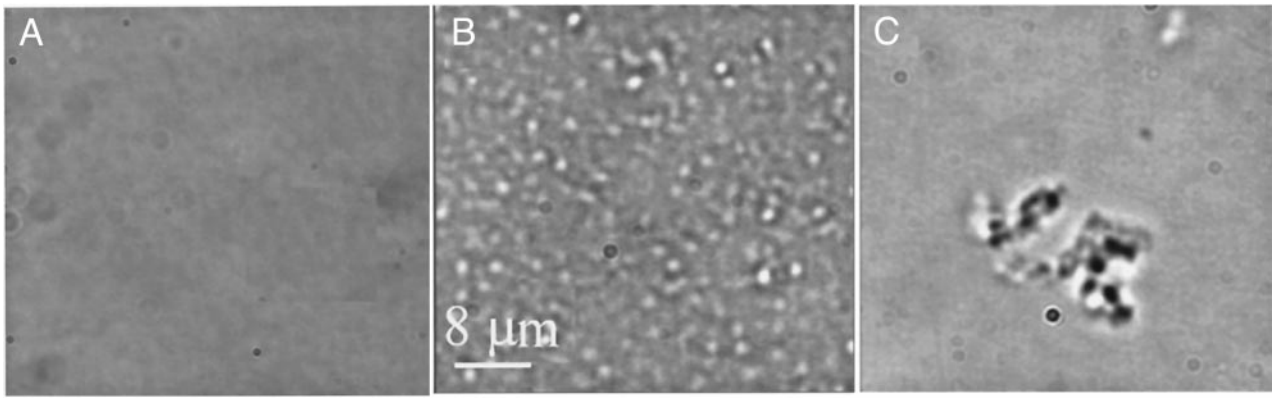

FIGURE 1 Aggregation of oxidized LDL in solution. LDL (0.2 mg/ml in phosphate buffer, pH 7.2) oxidized with hydrogen peroxide (88 mM) was analyzed with DVM. (*a*) LDL solution is clear initially. DVM cannot detect individual LDL molecules. (*b*) After 12 h of oxidation, >500 nucleation units, shown as *white spheres*, were found under the observation window, mostly near the surface of the glass coverslip. (*c*) After 24 h of reaction, nucleation units were chained together linearly. A representative coiled linear aggregate is shown.

Oxidation-induced LDL aggregation

Formation of nucleation units

When newly prepared LDL was incubated with H_2O_2, the solution was first clear (Fig. 1 *a*). After 12 h of incubation at room temperature, >500 nucleation units were found under the same observation window (~500 particles/1000 μm^3, Fig. 1 *b*). LDL stored at 4°C for ~2 months had approximately a couple dozen nucleation units in the window. We assumed that they were the lipid droplets reported in the literature (Guyton and Klemp 1989; Chao et al., 1990; Tertov et al., 1992; Hoff et al., 1992).

Formation of linear aggregates and fractals

Linear aggregates varied in size and shape. Linear aggregates of micron length, formed by the nucleation units, appeared after 1 day's reaction, ~20–50 of them in a window of 10,000 × 40 μm^2 (~1 to 3 particles/10,000 μm^3). These linear aggregates were short and consisted of <100 nucleation units. Most of them were coiled, especially those containing 20 or more nucleation units. The coils appeared rigid and stable. Unfolding of the coils was never observed. Representatives of the linear aggregates are shown (Fig. 1 *c*; Fig. 2, *a–f*). Some of the linear aggregates, especially those consisting of <20, but >6–8 nucleation units, were uncoiled, and their linear chains were twisted and bent continuously (Fig. 2, *a* and *b*). Others are more coiled than others (*c* and *d* vs. *a* and *b*). The aggregates in Fig. 2, *e* and *f* seem to be two linear aggregates twisted together. The coiled aggregates generally drifted in solution as compared with the fast-moving linear aggregates consisting of less than five nucleation units.

Fractals began to appear after 1 day of oxidation, but became the most common structures after 2 days. Small fractals seemed to be the products of branching of the linear

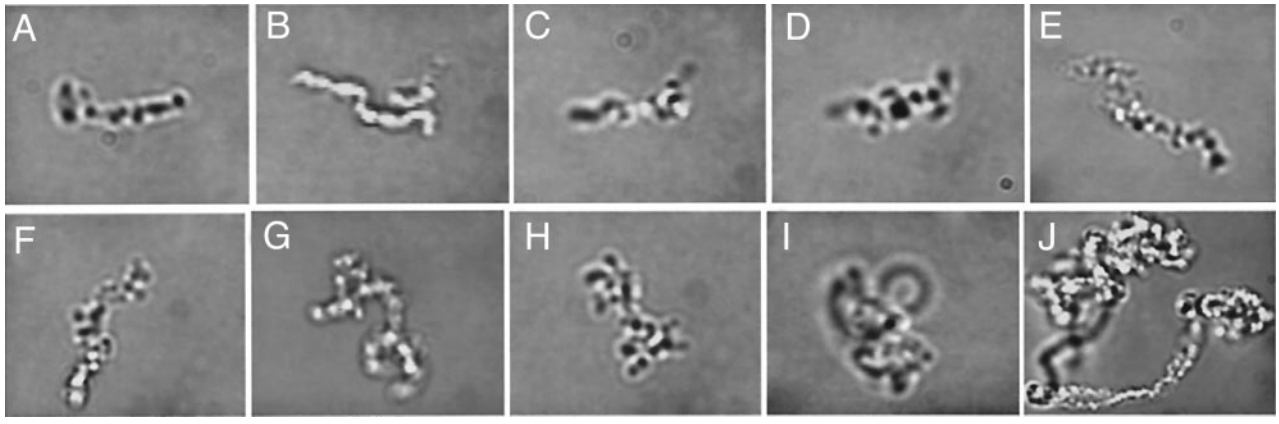

FIGURE 2 Linear aggregates and small fractals. Representatives of linear aggregates and small fractals are shown. (*a–d*) Linear aggregates. (*e* and *f*) Linear aggregates appear twisted against themselves. (*g* and *h*) Branching of the linear aggregates or small fractals. (*i* and *j*) A combination of linear, coiled, and possibly branching aggregates.

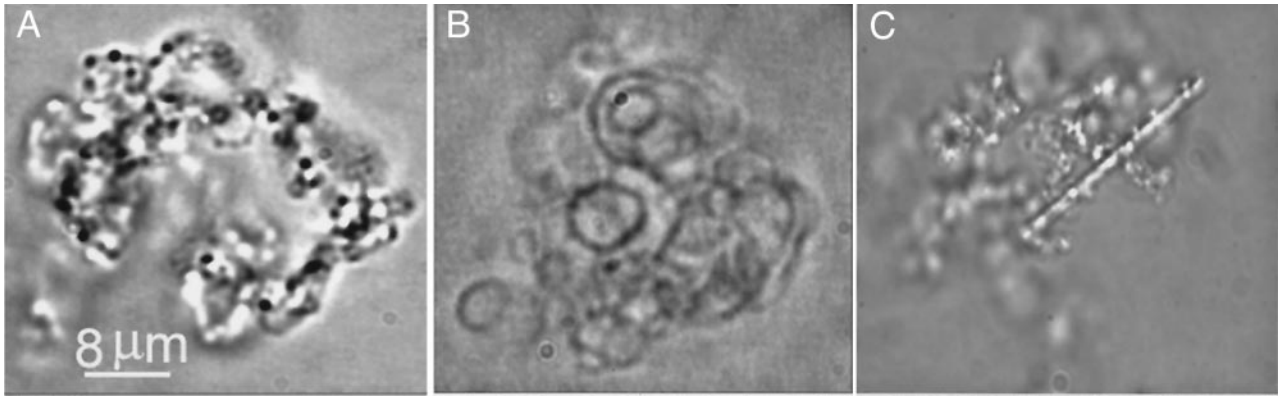

FIGURE 3 Fusion of LDL aggregates. (*a*) After 48 h of the reaction, the linear aggregates grew larger or assembled together and formed fractals. Vortex-induced aggregates had the same appearance as those induced by oxidation. (*b*) On the third day of reaction, adjacent nucleation units in a fractal have fused together into various-sized vesicles. The vesicles were attached to one another initially and then either broke apart or deposited onto the glass coverslip surface. Often, vesicles had nucleation units or small vesicles trapped inside. (*c*) A rod was found to have evolved from the fractal. The rod was rigid and straight and had a rough surface, which suggests a result of 1-D aggregation of adjacent nucleation units in the fractal. Scale bar: 8 μm for *a–c*.

aggregates (Fig. 2, *g* and *h*). Large fractals might have grown from the small fractals or resulted from random tangling among many small fractals (Fig. 2 *j*, Fig. 3 *a*). It was also quite common to observe two or more fractals interacting with one another. The fractals varied greatly in size from no more than 12 to more than 1000 nucleation units (Fig. 2, *a–j*, Fig. 3 *a*), if one could regard a linear aggregate as a special fractal.

We regard the process of converting monomeric LDL to fractals as an aggregation stage. At this stage, individual nucleation units retained their physical shape, as compared with a fusion stage as described below. The short linear aggregates and the fractals were built upon the nucleation units, which were the true basic units, generally referred to as nucleation units in colloidal science (Jullien and Botet, 1987) and as we also described in amyloid fiber formation (Xu et al., 2001). Similar to the basic units involved in the aggregation of other colloidal particles, the nucleation units of LDL also seem to be compact, in contrast to the amorphous structure observed for the fractals.

Continuous aggregation and fusion of fractals

On the third day, the density of the nucleation units decreased significantly, and fused vesicles 3–20 μm in diameter began to appear in solution. Most of the fused vesicles remained attached either to the fractals or to one another and absorbed less light than did the nucleation units and fractals (Fig. 3). We always observed more fractals than free vesicles suspended in solution, which suggests that either the rate at which the vesicles were formed was lower than that of the formation of the fractals or the rate at which the vesicles were deposited onto the glass surface was higher than that for the fractals, as discussed below.

Formation of spherical and tubular membrane vesicles

Intermediate steps of vesicle formation were also identified. Initially, the adjacent nucleation units may fuse with one another and form curved membrane surfaces, as shown in Fig. 4 *a*. These adjacent nucleation units may be distant from one another in the linear chain, but close together in space. These curved membrane surfaces, which remain attached to one another and to the fractals, form one or more irregular membranes, with a portion of a macroaggregate bound to the junction region between different curved surfaces (Fig. 4 *a*). These irregular membranes might serve as the base for the formation of singular or multiple vesicles. At this stage, the vesicle was generally attached to the fractals. The newly formed vesicles often have trapped inside them some nucleation units or portions of fractals (Fig. 4 *b*).

At the end of the third day, only a few small nucleation units were found trapped inside the vesicles, presumably because of their fusion with the membrane. The trapped portion of the macroaggregate generally remained motionless and was probably attached to the membrane wall and/or to the rest of the macroaggregate. Free vesicles with nucleation units or portions of fractals bound to the exterior were also quite common (Fig. 4 *c*). Eventually, these particles attached to the exterior of the vesicle disappeared, possibly being integrated into the membrane and becoming part of the spherical membrane vesicle. Membrane vesicles have been identified and isolated from the atherosclerotic plaques. These in vitro studies of LDL aggregation allow us to propose a theory of how these membrane vesicles might be formed in vivo.

In addition to the spherical vesicle formation, we occasionally observed some tubular vesicles (Fig. 4 *d*). They were attached exclusively to the fractals and were much less common than the spherical vesicles and the membrane

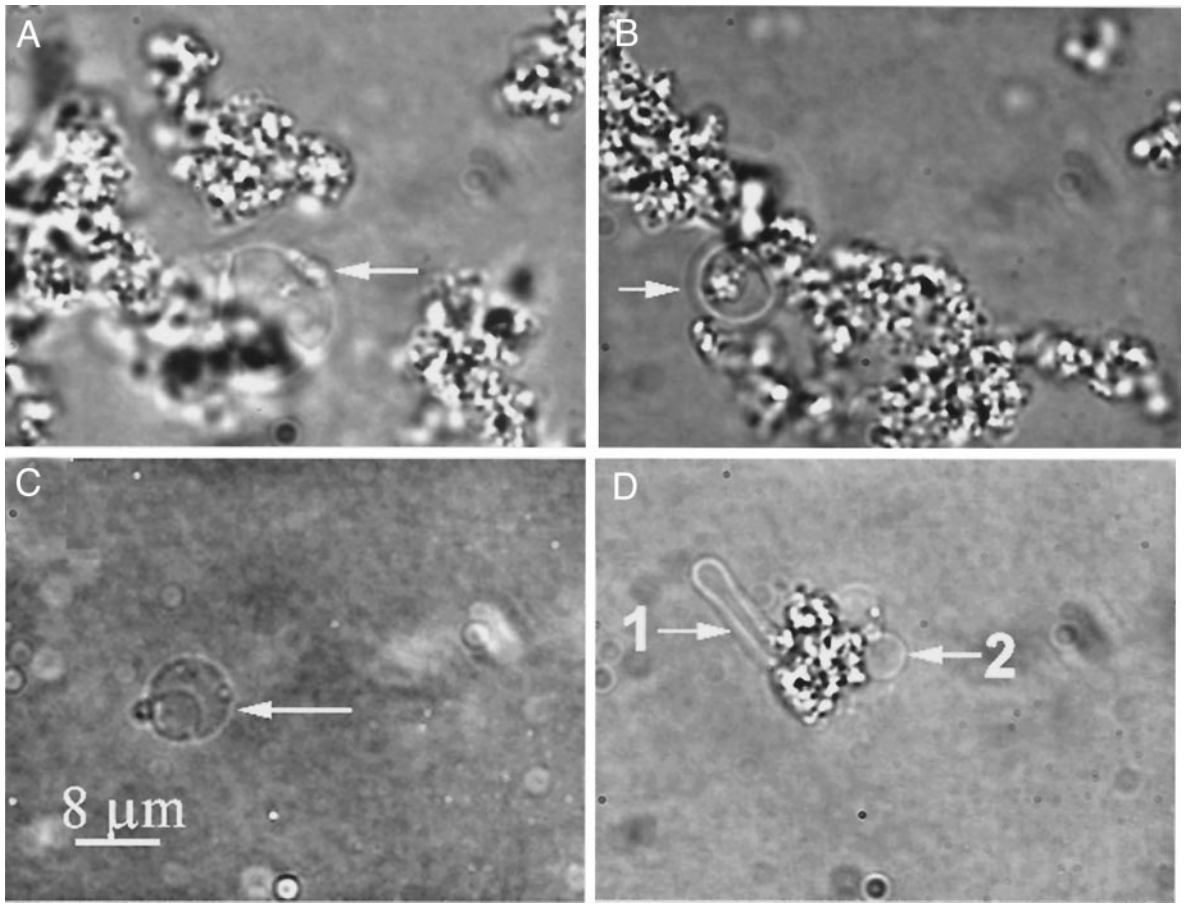

FIGURE 4 Membrane vesicle formation. Intermediate steps of vesicle formation were identified. Initially, the neighboring fractals fused into curved membrane surfaces (*arrow* in *a*). These surface curvatures often had nucleation units or portions of fractals attached to the junction region of the membranes. Continuous fusion of these curved membrane surfaces resulted in the formation of spherical membrane vesicles (*arrow* in *b*), which remained attached to the fractals or other vesicles initially and broke apart at the end (*arrow* in *c* and *2* in *d*). Vesicles free in bulk solution sometimes have trapped some nucleation units and small vesicles inside (*c*). Occasionally, tubular membrane vesicles were formed from the fractals (*arrow 1* in *d*). They were usually found attached to the fractals. Scale bar: 8 μm for *a–d*.

ribbons. Thus, the tubular membrane vesicles had evolved from the fractals as well. We hardly ever observed tubular vesicles free in bulk solution, which suggests that the tubular vesicles are unstable. No tubular vesicles trapped nucleation units or other aggregation intermediates.

Formation of membrane ribbons

Membrane ribbons were found in the oxidized LDL aggregates. They were approximately one-third as common as the spherical vesicles. Several kinds of intermediates appeared in the process of membrane ribbon formation. The first to appear in solution were solid, straight rods, which seemed to be formed by the linear aggregation of nearby nucleation units in a fractal (Fig. 5 *a*). The newly formed rods remained attached to the fractal and had a rather rough surface with surface contours. With time, the rods broke apart from the fractal, as shown in Fig. 5 *b*, with fragmented fractals spread along the rod. Once free, the rod started to flatten out and changed into a rough ribbon with a surface contour which is named after its characteristic rough surface as shown in Fig. 5 *c*. Bending and twisting of the rough ribbon was constantly observed, a reflection of the thermal motion of the fluid-like aggregates typically found during aggregation of amphipathic molecules (Israelachvili, 1994). The continuous fusion of the nucleation units of the rough ribbon resulted in the formation of a membrane ribbon, which had a characteristic smooth surface without surface contours and was capable of bending and twisting, as did the rough ribbon (Fig. 5 *d*).

The conversion of the fractals to spherical and tubular membrane vesicles and membrane ribbons was regarded as the fusion stage. The characteristics of this stage were the loss of the physical shape of the nucleation units and their transformation into membrane-like structures.

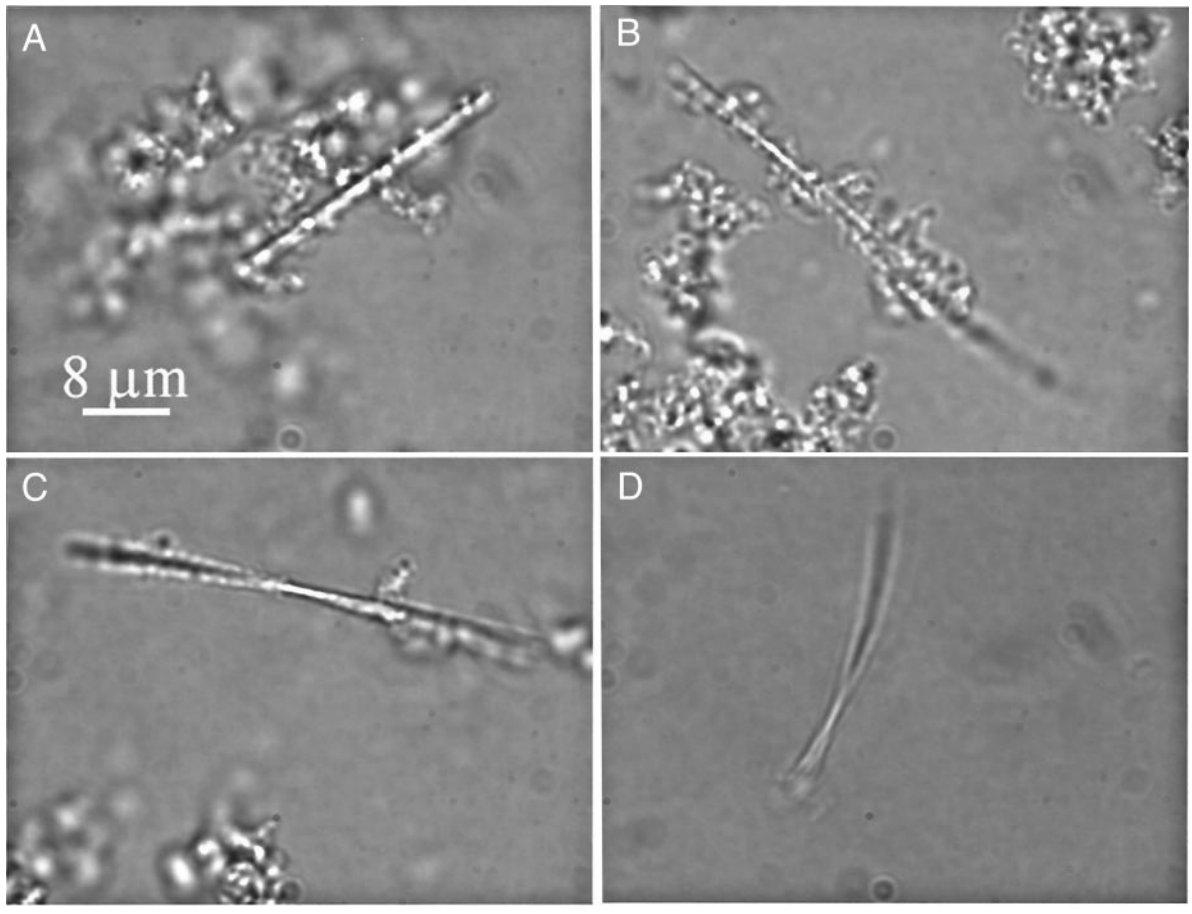

FIGURE 5 Formation of a membrane ribbon. Various intermediates in the formation of the membrane ribbon were observed. The specimen was prepared as in Fig. 1. (*a*) A rod was formed and remained attached to the fractals. The rod was straight, with a rough surface. (*b*) A rod was detached from the fractals and was free in bulk solution. Clusters of nucleation units remained bound to the rod. The surface of the rod remained rough. (*c*) A ribbon was formed from a rod. Some clusters of nucleation units were bound to the ribbon. The surface of the ribbon remained rough. (*d*) A membrane ribbon with a smooth surface was formed. The ribbon was free of attached nucleation units and was capable of bending and twisting. Scale bar: 8 μm for *a–d*.

Adsorption of lipoprotein aggregates to glass surfaces

On the fourth day, none of the aggregation intermediates could be detected in suspension. In contrast, deposition of the LDL and its aggregates or the fusion product on the glass coverslips increased dramatically. On day 4, the entire glass surface was covered with fused membranes, as compared with day 1, when only a portion of the glass surface ($<$10%) seemed to be covered.

Certain forms of aggregates were preferentially adsorbed to the glass surface (Fig. 6). The microaggregates, the short linear aggregates, and the membrane vesicles were adsorbed efficiently. The microaggregates were deposited as a dense but homogeneous monolayer (Fig. 6 *a*). The short linear aggregates were adsorbed to the glass substrate less efficiently than were the microaggregates. Most of these adsorbed linear aggregates consisted of $<$20 microaggregates (Fig. 6 *b*). A few fractals were also identified. They were adsorbed poorly to the glass coverslip (Fig. 6 *c*). The advanced aggregation products were mostly deposited as fused membranes. Various intermediates are shown in Fig. 6 *d*, where nucleation units, short linear aggregates and fractals, and the unilamellar and multilamellar membrane vesicles can be identified.

Alternative perturbations

We repeated the above experiments five times. No LDL aggregation was observed during a 5-day incubation of LDL in the absence of oxidant or the absence of other perturbations. Vortexing of LDL for 1 min resulted in fractal formation immediately, as shown in Fig. 3 *a*. Acidic pH (citrate buffer, pH 4.0), Ca^{2+} (5 mM $CaCl_2$), or Cu^{2+} (0.5 mM $CuSO_4$) led to LDL aggregation and fusion in a pathway similar to that of oxidation. The vortexing, acidic pH, and Ca^{2+} treatments were repeated three times. We also incu-

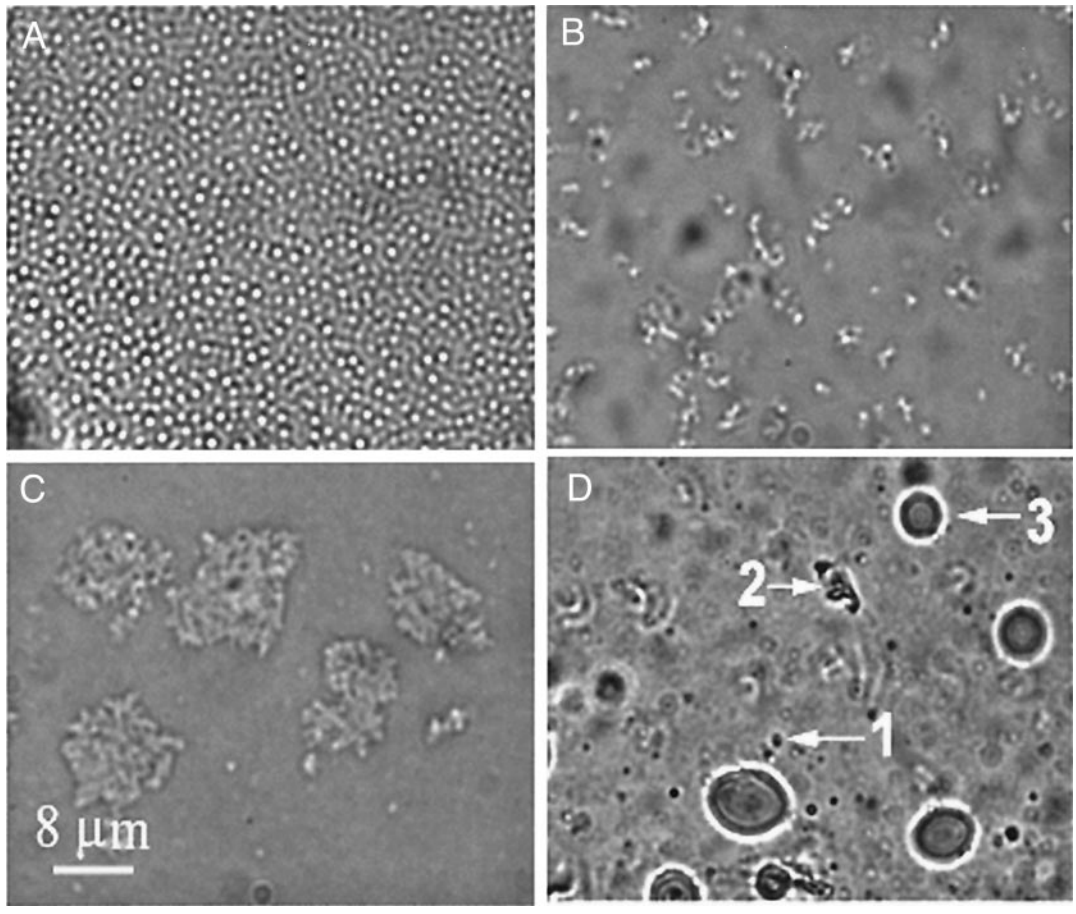

FIGURE 6 Oxidation-induced LDL aggregation intermediates deposited on glass coverslips were analyzed. The specimen was prepared as in Fig. 1 by an incubation of LDL with H_2O_2. (*a*) After 1 day of incubation, large spheres or nucleation units were found on the glass surface. (*b*) After 2 days of oxidation, linear aggregates were formed. (*c*) After 3 days of oxidation, fractals were found on the glass surface. (*d*) After 4 days of oxidation, a variety of aggregates were found deposited on the glass surface, including nucleation units (*1*), linear aggregates (*2*), and vesicles (*3*).

bated LDL with less H_2O_2, Ca^{2+}, or Cu^{2+} (at concentrations 10- and 100-fold less than what was used in oxidation-induced LDL aggregation) and found that the aggregation was slowed down significantly. It would take weeks to finish an aggregation reaction, which follows a pathway similar to what we observed above for H_2O_2 incubation.

TEM of oxidized lipoproteins

TEM images of these LDL aggregates induced by oxidation furnished results similar to those described above with DVM. Monomeric LDLs (*A*), nucleation units (*B*), fractals (*C*), and fused membrane vesicles (*D*) were observed under TEM with uranyl acetate stain, as shown in Fig. 7. Under our experimental conditions, the nucleation units deviated from a round shape and were approximately 4 to 6 times larger than the monomeric LDL particles (*A*).

DISCUSSION

The pathogenesis of atherosclerosis is an object of intensive study. It is clear that atherosclerotic heart disease is related to elevation in plasma LDL cholesterol, although the precise mechanistic relationship between the latter and the pathogenesis of atherosclerosis is still unknown (Guyton and Gotto, 1992). A widely held hypothesis is that, in the event of an artery leakage, the lipoprotein entering the blood vessel wall is subject to modification by oxidants, and the oxidized LDL sets in motion many of the cellular responses characteristic of atherosclerosis (Berliner and Heinecke, 1996). Included in the early responses of an elevated plasma LDL concentration is the presence of LDL aggregates at sites of potential atherosclerotic plaque development. In this study, we showed the effect of LDL oxidation by H_2O_2 on its aggregation capacity. The method used here enabled us to follow the aggregation pathway in solution.

We identified nine potential intermediates generated by oxidation-induced LDL aggregation and revealed the aggregation process (Fig. 8). Under the experimental conditions used, the nucleation units appeared in solution first, followed by linear aggregates, and then fractals. Curved membrane vesicles and tubular membrane vesicles and rods appeared in solution at about the same time and were

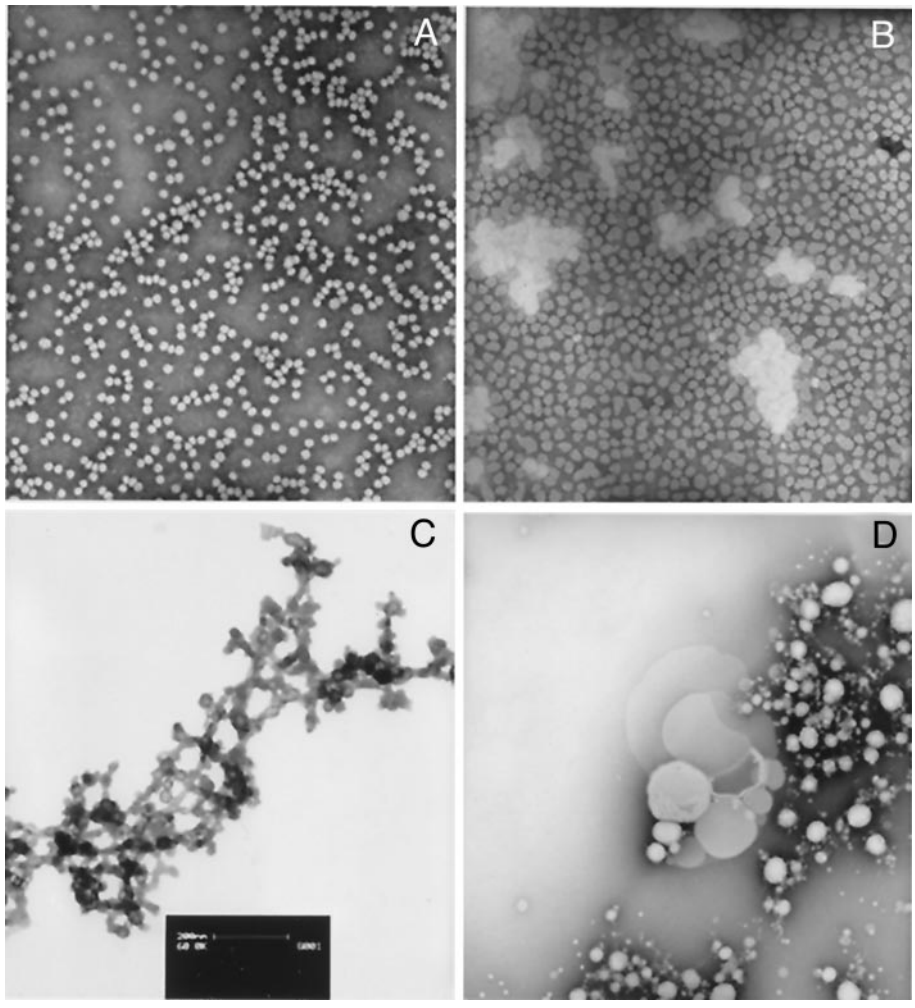

FIGURE 7 TEM analysis of oxidized LDL. LDL (30 μl, 0.2 mg/ml in 10 mM sodium phosphate, 150 mM NaCl, 0.02% NaN_3, pH 7.2) was incubated with H_2O_2 (88 mM). Specimens (3 μl) were removed after the oxidation reaction carried out for various times, deposited on a carbon grid, and uranyl acetate-stained. (*A*) Specimen before incubation with H_2O_2, where monomeric LDL was found. (*B*) Specimen from day 1, when nucleation units were found. (*C*) Specimen from day 2, when fractals were found. (*D*) Specimen from day 3, when fused membrane vesicles were found.

believed to be the product of further aggregation and fusion of adjacent nucleation units in the fractals. Whereas the curved membrane surfaces developed into spherical vesicles, the rods flattened out to rough and then to smooth ribbons. The spherical vesicles were more abundant than the membrane ribbons and the tubular membrane vesicles. Spherical vesicles often trapped inside some nucleation units or a portion of a macroaggregate. These vesicles could be unilamellar or multilamellar. Acidic conditions, calcium ions, or cuprous ions could also induce LDL aggregation and fusion, which seemed to follow a pathway similar to that induced by oxidation. Structural features such as the short linear aggregates, the fractals, the rods, the rough and smooth ribbons, and the tubular membrane vesicles were identified for the first time as intermediates of LDL aggregation.

LDL aggregation can be divided into two stages, aggregation and fusion. The aggregation stage encompasses the entire process of converting native LDL to fractals (steps 1 to 3 in Fig. 8), which is compatible with the amyloid fiber formation and aggregation of colloidal particles (Jullien and Botet, 1987; Xu et al., unpublished data). The fusion stage includes the formation of rods, curved membrane surfaces, membrane ribbons, and spherical and tubular membrane vesicles (steps 4 and 5). This stage is not observed in amyloid fiber formation, nor in normal colloidal aggregation. The fusion stage is thought to be characteristic of lipoproteins, which are rich in small amphipathic lipid and fatty acid molecules. These small amphipathic molecules are absent from amyloidogenic proteins.

The aggregation of LDL resembles a chemical colloidal aggregation, a well-understood process. Colloidal aggregation can be induced by a change in the surface electric property of the particles. Oxidation might have resulted in a change in the surface chemical potential of the LDL particles, which led to the aggregation of monomeric LDL to

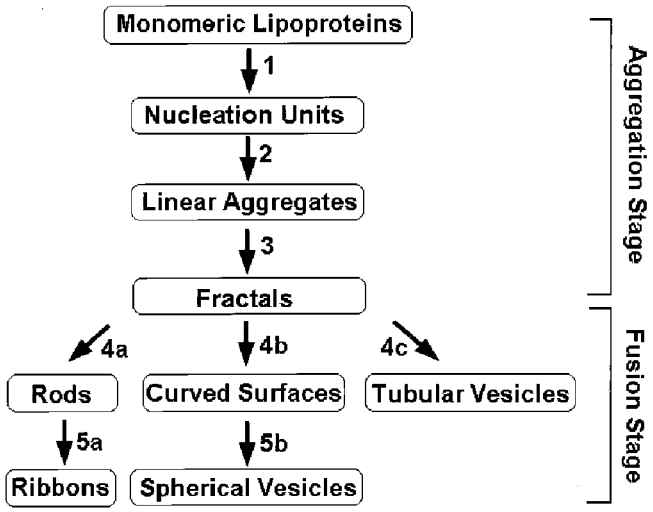

FIGURE 8 Schematic representation of the mechanism of LDL aggregation induced by oxidation. The oxidized LDL molecules aggregate and form nucleation units (step 1 in this figure and in Fig. 1 *b*). Nucleation units then assemble into a chained structure that often is coiled (step 2 in this figure and in Figs. 1 *c*, 2, *c* and *d*). These linear aggregates then either branch or become tangled with one another and form fractals (step 3 in this figure and in Figs. 2, *g* and *h*, and 3 *a*). The adjacent nucleation units in the fractals then fuse with one another and form either 1-D rods (step 4a in this figure and Fig. 5 *a*) or curved membrane surfaces (step 4b in this figure and Fig. 4 *a*). The rod slowly evolves into a rough ribbon initially and then into a smooth membrane ribbon (step 5a in this figure and Fig. 5, *b–d*), whereas the curved membrane surface continually fuses with other nucleation units in the fractal, forming spherical membrane vesicles (step 5b in this figure, Figs. 3 *b*, 4, *b* and *c*). Tubular membrane vesicles are formed rarely from the fractals (step 4c in this figure and Fig. 4 *d*).

nucleation units (step 1 in Fig. 8). Linear aggregation and fractal formation are results of further aggregation of the nucleation units, similar to what we observed for amyloid fibers. Fusion of the neighboring nucleation units in the fractals results in the formation of membrane curvatures and vesicles. Formation of rods might be a result of dipole-dipole interaction of nucleation units in the fractals. Fusion of the nucleation units in the rods leads to the formation of membrane ribbons.

Oxidation of LDL could lead to a reduction of the LDL surface charge density. The oxidized cholesterol esters and triglycerides are more polar and amphipathic than their precursors; it would be energetically less stable for them to remain in the hydrophobic region of LDL. Migration of these oxidized molecules from the hydrophobic region to or near the surface of LDL reduces the surface charge density and then the surface electric potential of the lipoproteins, and leads to LDL aggregation. For example, the oxidation of the PUFA molecules may play a leading role in such a reduction of the surface charge density. The aldehydes, derived from breakage of the nonpolar side of the ethyl bond of a fatty acid, would migrate to the surface of the LDL because of the polarity of the aldehyde group and its capability of forming hydrogen bonds. The hydroxy- or peroxy-fatty acids would reposition themselves so that both the hydroxyl or peroxyl group and the carboxyl group would reside in the polar and charged head-group region (Kellner and Cadenhead, 1977, 1978). The arrival of these aldehyde, hydroxyl, and peroxyl groups at the head-group region would occupy more space without additional charges and thus reduce the charge density.

The chemistry of LDL oxidation has been studied extensively. Many small molecules in LDL, including those in the hydrophobic core, are vulnerable to oxidants. The following oxidation reactions have been observed: β-carotene to retinol and retinoic acid, α-tocopherol to α-tocopherol hydroquinone, PUFA to hydroxy- and peroxy-fatty acids and other derivatives including malondialdehyde and other short-chain aldehydes, ubiquinol to ubiquinone, and cholesterol to cholesterol oxides (Rice-Evans and Bruckdorfer, 1992). The aldehydes formed could react with amine in apoB and lead to cross-linking of lysine residues at different regions of apoB. Such a type of lipid/protein conjugation has been detected for 4-hydroxy-2-nonenal-modified histidine, lysine, and cysteine residues by amino acid analysis of oxidized LDL (Uchida et al., 1994). All the modifications affect the integrity of the structure of LDL and lead to the change in the LDL surface electric property that is often the cause of protein aggregation.

The oxidant concentrations used in these reactions, 88 mM H_2O_2 and 0.5 mM $CuSO_4$, are 50- to 100-fold higher than their physiologic concentrations. However, in vivo, lipoprotein aggregation and deposition in arteries occur over a period of decades, and it is thus impractical to use oxidants at their physiologic concentration for in vitro studies. Oxidizing lipoproteins under physiologic conditions in plasma (0.5 mM H_2O_2 or 10 μM $CuSO_4$) resulted in no discernible reaction over a period of 10 days. In contrast, LDL trapped in the subendothelia is taken up by macrophages. The oxidant concentration inside a macrophage is much higher than that in the subendothelia. Moreover, a relative deficiency of lysosomal hydrolysis of lipoproteins in proportion to the lipoprotein load presented to the lysosome might lead to lysosomal lipoprotein accumulation (Shio et al. 1978; Fowler et al., 1980). An acidic environment in lysosomes is optimal for lipoprotein aggregation. The oxidized LDL is toxic, which may be responsible for the deficiency of enzymes in the lysosomes in degrading LDL.

Similar to H_2O_2, Cu^{2+} is also an oxidant that is capable of inducing LDL aggregation by oxidizing some of the molecules in LDL. In addition, as a dication, Cu^{2+} can be adsorbed to the negatively charged LDL surface and affect the surface electric potential of LDL directly, as is also the case for Ca^{2+}. The acid or Ca^{2+} treatment directly affects the surface potential of LDL and leads to LDL aggregation (Jullien and Botet, 1987; Israelachvili, 1994; Myers, 1990). Acid neutralized the carboxyl groups and then decreased the net negative charge of LDL, whereas a small change in the dication concentration, such as calcium ions, would greatly

affect the surface potential of LDL and then the property of the molecule (McLaughlin, 1977; Honig et al., 1986). Agitation (thermal or vortexing) yielded particles with more kinetic energy to overcome the electric potential barrier to aggregation (Jullien and Botet, 1987).

CONCLUSION

It seems that a fundamental similarity and parallel exists between the aggregation of lipoproteins and amyloid proteins. Both aggregate and form large spheres or nucleation units initially. These nucleation units, in turn, assemble linearly. Amyloid fibers tend to be straight, whereas linear aggregates of lipoproteins tend to be coiled. Lipoprotein aggregates grow into fractals, whereas few branches exist in amyloid fibers. Nevertheless, the aggregation stage of lipoproteins resembles the amyloid fiber formation, and both seem to follow the physical law derived for colloidal particle aggregation. Particles aggregate and form large spheres to minimize surface energy, and the large spheres aggregate and form fractals (Winslow, 1949; Witten and Sander, 1981; Meakin, 1983; Halsey, 1993; Halsey et al., 1997). Unlike the case of amyloid fibers, apparent structural evolution continues from the fractals of lipoproteins to membrane vesicles and ribbons. These differences could be a result of the different composition of these two proteins. Lipoproteins are composed of lipids, fatty acids, cholesterols, and others in addition to polypeptides. The fusion of the neighboring nucleation units in the fractals reflects the presence of these amphipathic molecules in lipoprotein aggregates.

We thank Dr. Stuart A. Rice for the use of his laboratory for the DVM experiments. We are grateful to Erica Reschly and Dr. Godfrey S. Getz for helpful discussions and for providing some of the LDL used in the experiments. We also thank Dr. Morton F. Arnsdorf for his support of the work in which we used imaging techniques to study lipoproteins. This work is supported in part by a grant from the University of Chicago-Argonne National Laboratory Collaborative grant Programs and by National Institutes of Health grant R44GM/HL56056.

REFERENCES

Adriani, P. M., and A. P. Gast. 1990. Electric-field-induced aggregation in dilute colloidal suspensions. *Faraday Discussions Chem. Soc.* 90:17–29.

Belkner, J., R. Wiesner, J. Rathman, J. Barnett, E. Sigal, and H. Kuhn. 1993. Oxygenation of lipoproteins by mammalian lipoxygenases. *Eur. J. Biochem.* 213:251–261.

Berliner, J. A., and J. W. Heinecke. 1996. The role of oxidized lipoproteins in atherosclerosis. *Free Radical Biol. Med.* 20:707–727.

Binnig, G., C. F. Quate, and C. Gerber. 1986. Atomic force microscope. *Phys. Rev. Lett.* 56:930–933.

Bolgar, M. S., C. Y. Yang, and S. J. Gaskell. 1996. First direct evidence for lipid/protein conjugation in oxidized human low density lipoprotein. *J. Biol. Chem.* 271:27999–28001.

Camejo, G. 1982. The interaction of lipids and lipoproteins with the intercellular matrix of arterial tissue: its possible role in atherosclerosis. *Adv. Lipid Res.* 19:1–53.

Chao, F. F., E. J. Blanchette-Mackie, Y. J. Chen, B. F. Dickens, E. Berlin, L. M. Amende, S. I. Skarlatos, W. Gamble, J. H. Resau, W. T. Mergner, and H. S. Kruth. 1990. Characterization of two unique cholesterol-rich lipid particles isolated from human atherosclerotic lesions. *Am. J. Pathol.* 136:169–179.

Chao, F. F., E. J. Blanchette-Mackie, V. V. Tertov, S. I. Skarlatos, and Y. J. Chen. 1992. Hydrolysis of cholesterol ester in low density lipoprotein converts this lipoprotein to a liposome. *J. Biol. Chem.* 267:4992–4998.

Crocker, J. C., and D. G. Grier. 1996. Methods of digital microscopy for colloidal studies. *J. Colloid Interface Sci.* 179:298–310.

Fowler, S., P. A. Berberian, H. Shio, S. Goldfischer, and H. Wolinsky. 1980. Characterization of cell populations isolated from aortas of rhesus monkeys with experimental atherosclerosis. *Circ. Res.* 46:520–530.

Getz, G. S. 1990. An overview of atherosclerosis: a look to the future. *Toxicol. Pathol.* 18:623–635.

Guyton, J. R., and A. M. Gotto. 1992. *In* Vascular Medicine. chap. 12. J. Loscalzo, M. A. Creager, V. J. Dzau, editors. Little, Brown and Company, Boston, MA.

Guyton, J. R., and K. F. Klemp. 1989. The lipid-rich core region of human atherosclerotic fibrous plaques. Prevalence of small lipid droplets and vesicles by electron microscopy. *Am. J. Pathol.* 134:705–717.

Hakala, J. K., K. Oorni, K., M. Ala-Korpela, and P. T. Kovanen. 1999. Lipolytic modification of LDL by phopholipase A2 induces particle aggregation in the absence and function in the presence of heparin. *Arterioscler. Thromb. Vasc. Biol.* 19:1276–1283.

Hansma, P. K., V. B. Elings, O. Marti, and C. E. Bracker. 1988. Scanning tunneling microscopy and atomic force microscopy: application to biology and technology. *Science.* 242:209–216.

Halsey, T. C. 1993. Electrorheological fluids-structure and dynamics. *Adv. Materials.* 5:711–718.

Halsey, T. C., B. Duplantier, and K. Honda. 1997. Multifractal dimensions and their fluctuations in diffusion-limited aggregation. *Phys. Rev. Lett.* 78:1719–1722.

Herrmann, H. 1986. Geometrical cluster growth models and kinetic gelation. *Phys. Report.* 136:153–224.

Hoff, H. F., T. D. Whitaker, and J. O'Neil. 1992. Oxidation of low density lipoprotein leads to particle aggregation and altered macrophage recognition. *J. Biol. Chem.* 267:602–609.

Honig, B. H., W. L. Hubbell, and R. F. Flewelling. 1986. *Ann. Rev. Biophys. Chem.* 15:163–193.

Israelachvili, J. 1994. *In* Intermolecular and Surface Forces. Chaps. 5 and 16. J. Israelachvili, editor. Academic Press Inc., San Diego.

Jullien, R., and R. Botet. 1987. *In* Aggregates and Fractal Aggregates. Chap 1. R. Julien, R. Botet, editors. World Scientific Publishing Co., Singapore.

Jullien, R., H. Herrmann, M. Kolb, and J. Vannimenus. 1985. CECAM-workshop on kinetic models for cluster formation. *J. Stat. Phys.* 39: 241–246.

Kellner, B. M., and D. A. Cadenhead. 1977. Monolayer studies of hydroxyhexadecanoic acids. *J. Colloid Interface Sci.* 63:452–460.

Kellner, B. M., and D. A. Cadenhead. 1978. Monolayer studies of methyl hydroxyhexadecanoates. *Chem. Phys. Lip.* 23:41–48.

Khoo, J. C., E. Miller, P. McLoughlin, and D. Steinberg. 1990. Prevention of low density lipoprotein aggregation by high density lipoprotein or apolipoprotein A-I. *J. Lipid Res.* 31:645–652.

Koller, E. 1986. Lipoprotein binding proteins in the human platelet plasma membrane. *FEBS Lett.* 97–101.

Kumar, V., R. S. Cotran, and S. L. Robbins. 1997. *In* Basic Pathology. Chaps. 10, 14, and 16. V. Kumar, R. S. Coltan, and S. L. Robbins, editors. W. B. Saunders Company, Philadelphia.

Maor, I., and M. Aviram. 1999. Macrophage released proteoglycans are involved in cell-mediated aggregation of LDL. *Atherosclerosis.* 142: 57–66.

Marathe, S., G. Kuriakose, K. J. Williams, and I. Tabas. 1999. Sphingomyelinase, an enzyme implicated in atherosclerosis, is present in atherosclerotic lesions and binds to specific components of the subendothelial extracellular matrix. *Arterioscler. Thromb. Vasc. Biol.* 19: 2648–2658.

McLaughlin, S. 1977. Electrostatic potential at membrane-solution interfaces. *Curr. Top. Memb.* 9:71–144.

Meakin, P. 1983. Diffusion-controlled cluster formation in 2-dimensional space. *Phys. Rev. A.* 27:1495–1507.

Myers, D. 1990. *In* Surfaces, Interfaces, and Colloids. Chaps. 4 and 5. D. Myers, editor. VCH Publishers, Inc., New York.

Navab, M., J. A. Berliner, A. D. Watson, S. Y. Hama, M. C. Territo, A. J. Lusis, D. M. Shih, B. J. Van Lenten, J. S. Frank, L. L. Demer, P. A. Edwards, and A. M. Fogelman. 1996. The yin and yang of oxidation in the development of the fatty streak. *Arterioscler. Thromb. Vasc. Biol.* 16:831–842.

Rice-Evans, C., and K. R. Bruckdorfer. 1992. Free radicals, lipoproteins and cardiovascular dysfunction. *Mol. Aspects Med.* 13:1–111.

Sander, L. 1986. Fractal growth processes. *Nature.* 322:789–793.

Schumaker, V. N., and D. L. Puppione. 1986. Sequential flotation ultracentrifugation. *Methods Enzymol.* 128:155–170.

Shio, H., N. J. Haley, and S. Fowler. 1978. Characterization of lipid-laden aortic cells from cholesterol-fed rabbits. II. Morphometric analysis of lipid-filled lysosomes and lipid droplets in aortic cell populations. *Lab. Invest.* 39:390–397.

Tertov, V. V., A. N. Orekhov, I. A. Sobenin, Z. A. Gabbasov, E. G. Popov, A. A. Yaroslavov, and V. N. Smirnov. 1992. Three types of naturally occurring modified lipoproteins induce intracellular lipid accumulation due to lipoprotein aggregation. *Circ. Res.* 71:218–228.

Tirziu, D., A. Dobrian, C. Tasca, M. Simionescu, and N. Simionescu. 1995. Intimal thickenings of human aorta contain modified reassembled lipoproteins. *Atherosclerosis.* 112:101–114.

Uchida, K., S. Toyokuni, K. Nishikawa, S. Kawakishi, H. Oda, H. Hiai, and E. R. Stadtman. 1994. Michael addition-type 4-hydroxy-2-nonenal adducts in modified low-density lipoproteins: markers for atherosclerosis. *Biochemistry.* 33:12487–12494.

Winslow, W. 1949. Induced fibration of suspensions. *J. Appl. Phys.* 20: 1137–1145.

Witten, T. A., Jr., and L. M. Sander. 1981. Diffusion-limited aggregation, a kinetic critical phenomenon. *Phys. Rev. Lett.* 47:1400–1403.

Witztum, J. L., and D. Steinberg. 1991. Role of oxidized low density lipoprotein in atherogenesis. *J. Clin. Invest.* 88:1785–1792.

Xu, S. 1998. Apolipoprotein(a) binds to low-density lipoprotein at two distant sites in lipoprotein(a). *Biochemistry.* 37:9284–9294.

Xu, S., and M. F. Arnsdorf. 1994. Calibration of the scanning (atomic) force microscope with gold particles. *J. Microsc.* 173:199–210.

Xu, S., and M. F. Arnsdorf. 1995. Electrostatic force microscope for probing surface charges in aqueous solution. *Proc. Natl. Acad. Sci. U.S.A.* 92:10384–10388.

Xu, S., and M. F. Arnsdorf. 1997. Scanning (atomic) force microscopy imaging of earthworm haemoglobin calibrated with spherical colloidal gold particles. *J. Microsc.* 187:43–53.

Xu, S., B. J. Bevis, and M. F. Arnsdorf. 2001. The assembly of amyloidogenic yeast Sup35 as assessed by scanning (atomic) force microscopy: an analogy to linear colloidal aggregation? *Biophys. J.* 81:446–454.

Xu, X. X., and I. Tablas. 1991. Sphingomyelinase enhances low density lipoprotein uptake and ability to induce cholesterol ester accumulation in macrophages. *J. Biol. Chem.* 266:24849–24858.